COSMIC RAY ANISOTROPIES

Silvia Mollerach
Centro Atomico Bariloche
CONICET

MAIN QUESTION:

Nature and origin of UHECRs

OBSERVABLES:

- Spectrum

- Composition indicators like X_{max}

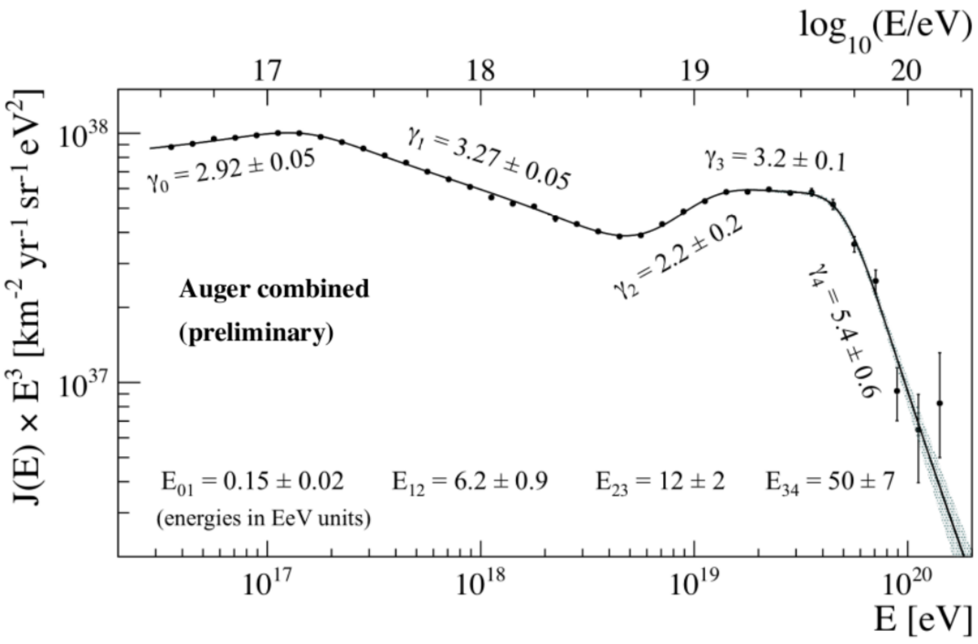

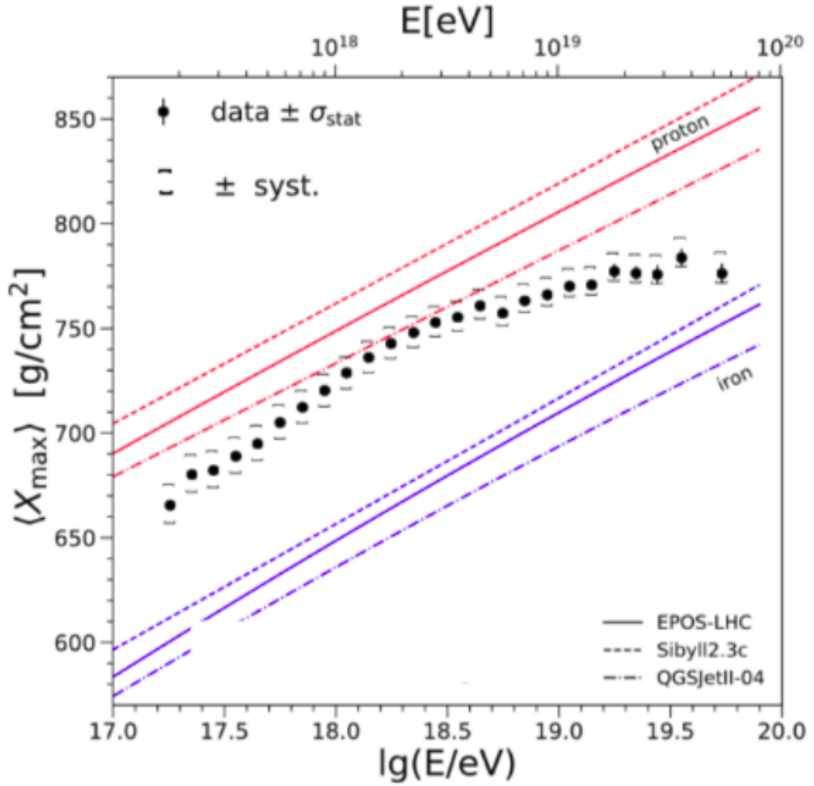

- Anisotropies in the arrival directions

BEST FIT OF SPECTRUM AND COMPOSITION OF UHECRs (above the ankle)

Simple model of sources continuously distributed and accelerating particles with rigidity dependent spectrum (power law with exponential cutoff)

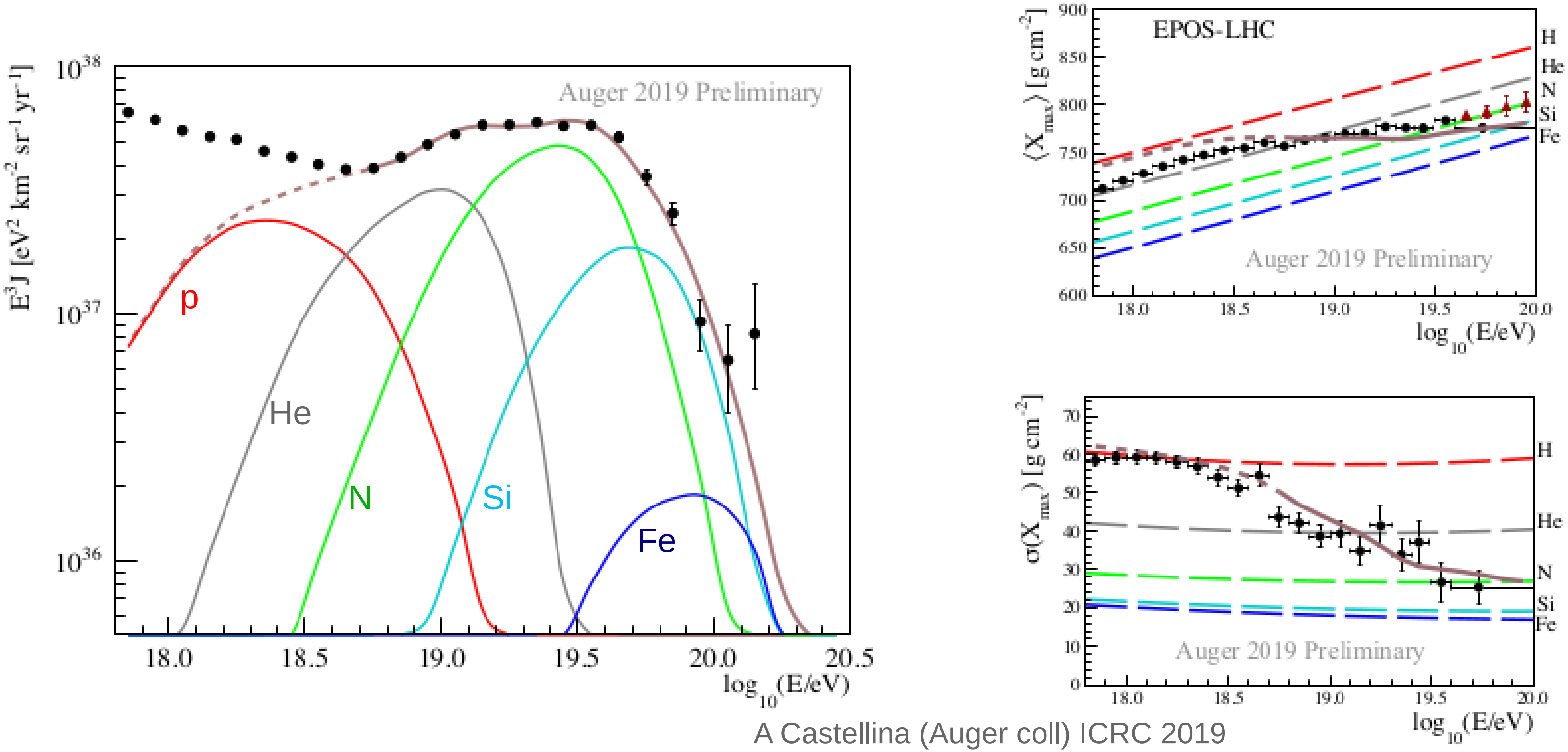

A Castellina (Auger coll) ICRC 2019

Auger favors mixed composition with hard rigidity dependent spectrum and low rigidity cutoff

$R_{cut} = E_{cut}/Z \sim 5$ EV

Final steepening of the spectrum is combination of propagation and maximum rigidity at the source

Interactions with radiation backgrounds:

Limit the distance from which UHECRs can reach us → at the highest energies sources cannot be too far away

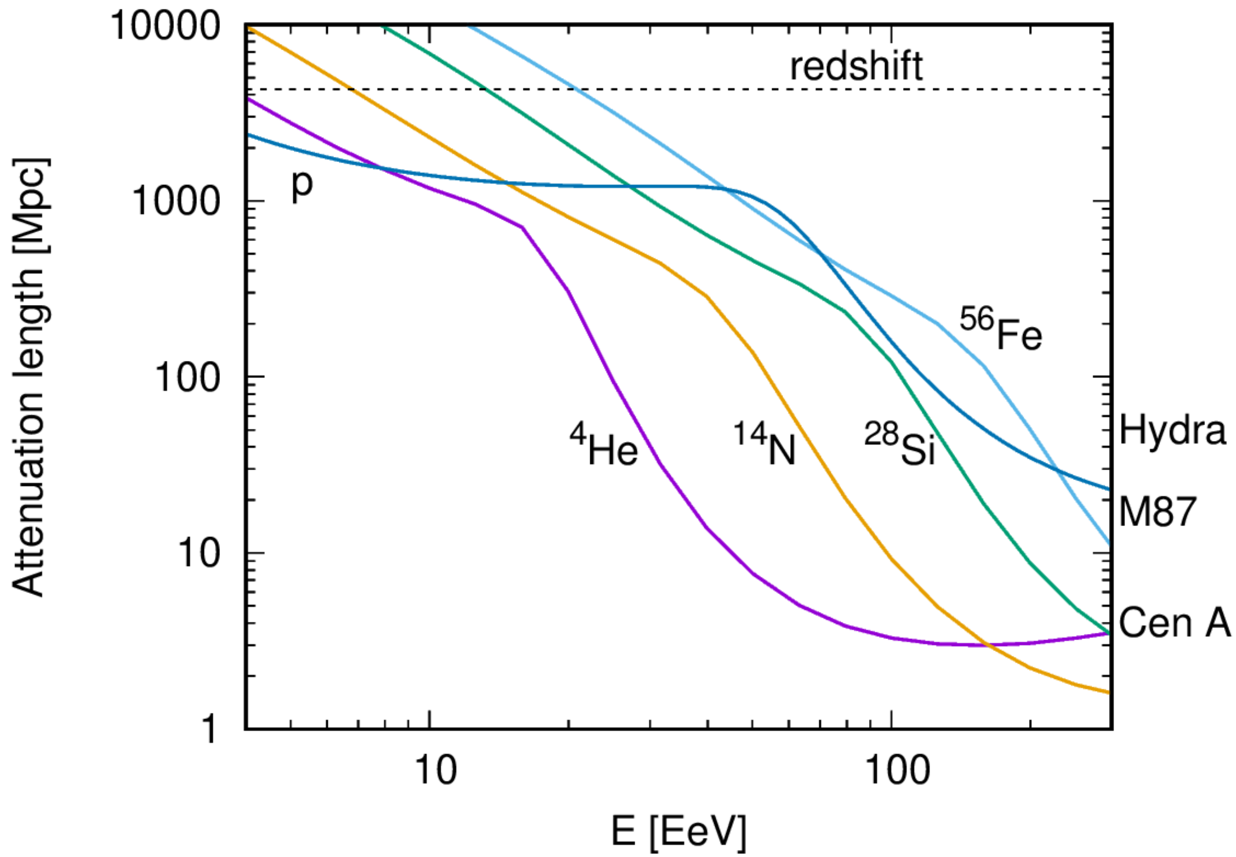

$$\lambda^{-1} = -\frac{1}{c}\frac{d\,lnE}{dt}$$

Main difficulty to identify UHECR sources: magnetic deflections

Regular B field: $\delta \simeq 10^{\circ} \frac{10\,\mathrm{EeV}}{E/Z} \left| \int_0^L \frac{d\vec{x}}{\mathrm{kpc}} \times \frac{\vec{B}}{2\,\mu\mathrm{G}} \right|$ Turbulent B field: $\delta_{\mathrm{rms}} \simeq \frac{BZe}{E}\sqrt{\frac{Ll_c}{2}} \simeq 4^{\circ} \frac{B}{\mathrm{nG}} \frac{10\,\mathrm{EeV}}{E/Z} \frac{\sqrt{Ll_c}}{\mathrm{Mpc}}$

Problem: Galactic and extragalactic magnetic fields are poorly know – composition is unknown

Arrival directions: affected by propagation in intervening magnetic fields → depends on energy and Z

$r_L = E/ZeB$

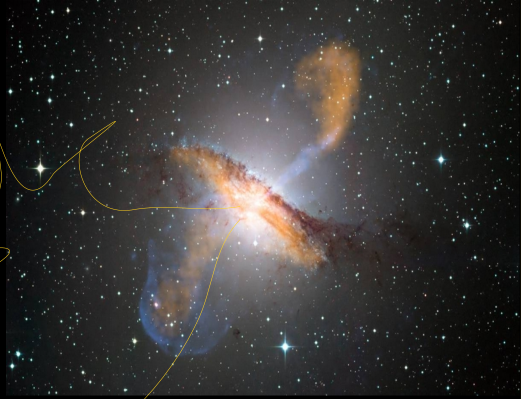

Diffusive or quasirectilinear?

- spectrum
- arrival directions distribution

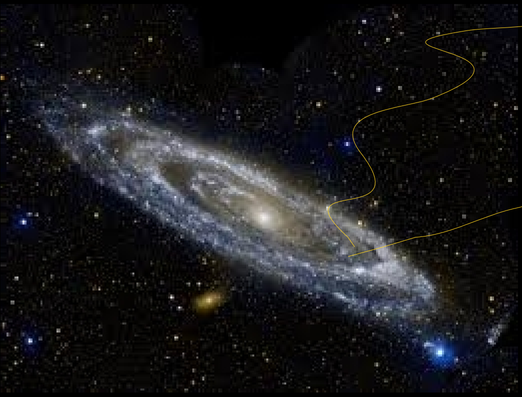

ANISOTROPY SEARCHES

Distribution of arrival directions expected to give additional clues to understand UHECRs

Large scale anisotropies:

Could signal galactic-extragalactic transition
- Galactic: diffusive escape from the Galaxy of galactic CRs
- Extragalactic: diffusive propagation in XG magnetic field from individual sources
  Anisotropies in the distribution of XG CR sources
- Small dipole due to our motion (Compton-Getting effect, below 1%).

- 3D anisotropies above full efficiency (E > 4 EeV): reconstruct full dipole (and quadrupole)
- anisotropies in right ascension at all energies (E > 0.03 EeV)

reconstruct equatorial dipole component, for which systematic effects under control

Small scale anisotropies:

Largest energies: above GZK CRs come from nearby sources and with small deflections for light composition component → trace source population

- search for excess of flux in different angular windows
- look for correlations with possible source populations

LARGE SCALE ANISOTROPIES: WEIGHTED FOURIER ANALYSIS

Account for spurious modulations of the flux:
- correct energy estimation for atmospheric conditions (temperature and pressure) and geomagnetic effect on air shower development
- weight w_i accounting for detector dead time and (small) tilt of the array

modulation in right ascension (x= α) and azimuth (x=Φ): Fourier coefficients of order k

$$a_k^x = \frac{2}{\mathcal{N}} \sum w_i \cos(kx_i) \ , \ b_k^x = \frac{2}{\mathcal{N}} \sum w_i \sin(kx_i)$$

$$r_k^x = \sqrt{(a_k^x)^2 + (b_k^x)^2}, \qquad \varphi_k^x = \frac{1}{k} \arctan \frac{b_k^x}{a_k^x}$$

amplitude　　phase

$$\mathcal{N} \equiv \textstyle\sum_i w_i$$

Weights:

$$w_i = [\Delta N_{\rm cell}(\alpha_i^0)(1 + 0.003 \tan\theta_i \cos(\phi_i - \phi_0))]^{-1}$$

number of active detector 'hexagons' (→ $\Delta N_{\rm cell}$)

right ascension of the zenith of the observatory (→ α_i^0)

event coordinates (→ θ_i, ϕ_i)

Average tilt of the array ϕ_0 = -30° (~South-East)

$$P(\geqslant r) = \exp(-\mathcal{N} r^2/4)$$

For dipolar modulation, $d_\perp \simeq \dfrac{r_1^\alpha}{\langle \cos\delta \rangle}$ **and** $d_z \simeq \dfrac{b_1^\phi}{\langle \sin\theta \rangle \cos l_{obs}}$

$$l_{obs} = -32.5^o$$

E > 4 EeV: SD1500 fully efficient up to 80° → cover 85% of the sky (dec < 45°)

3D dipole: equatorial dipole ($d_\perp$) , NS component (d_z) , total amplitude (d) and direction

Energy [EeV] interval	median	N	$d_\perp$	d_z	d	α_d [°]	δ_d [°]
4 - 8	5.0	88,325	$0.010^{+0.007}_{-0.004}$	-0.016 ± 0.009	$0.019^{+0.009}_{-0.006}$	69 ± 46	-57^{+24}_{-20}
≥ 8	11.5	36,928	$0.060^{+0.010}_{-0.009}$	-0.028 ± 0.014	$0.066^{+0.012}_{-0.008}$	98 ± 9	-25 ± 11
8 - 16	10.3	27,271	$0.056^{+0.012}_{-0.010}$	-0.011 ± 0.016	$0.057^{+0.014}_{-0.008}$	97 ± 12	-11 ± 16
16 - 32	20.2	7,664	$0.075^{+0.023}_{-0.018}$	-0.07 ± 0.03	$0.10^{+0.03}_{-0.02}$	80 ± 17	-44 ± 14
≥ 32	39.5	1,993	$0.13^{+0.05}_{-0.03}$	-0.09 ± 0.06	$0.16^{+0.06}_{-0.03}$	152 ± 19	-34^{+19}_{-20}

$$P = 1.4 \times 10^{-9} \ (6\sigma)$$

FLUX MAP FOR E > 8 EeV

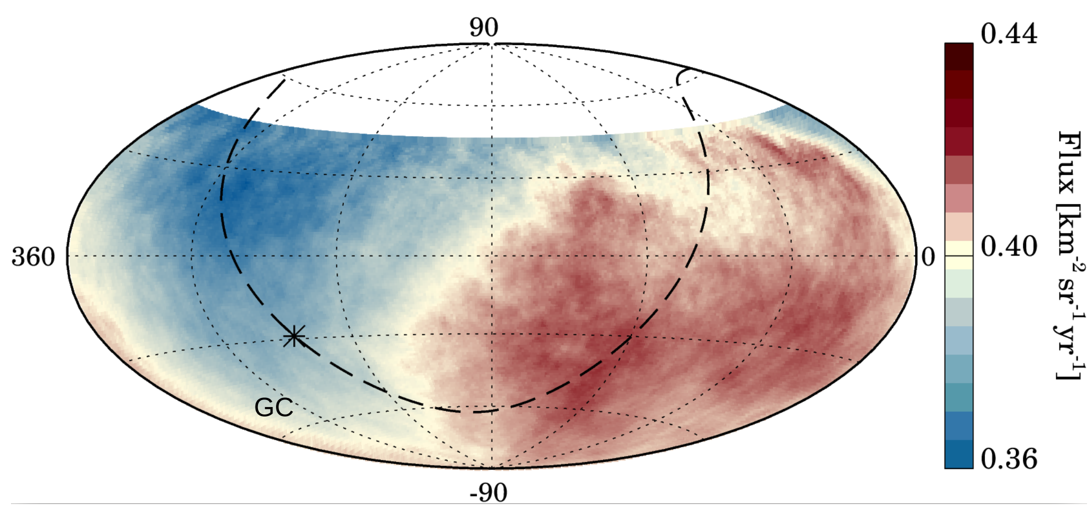

equatorial coordinates, smoothed on 45° radius windows

Energy dependence of dipolar modulation

ICRC 2019

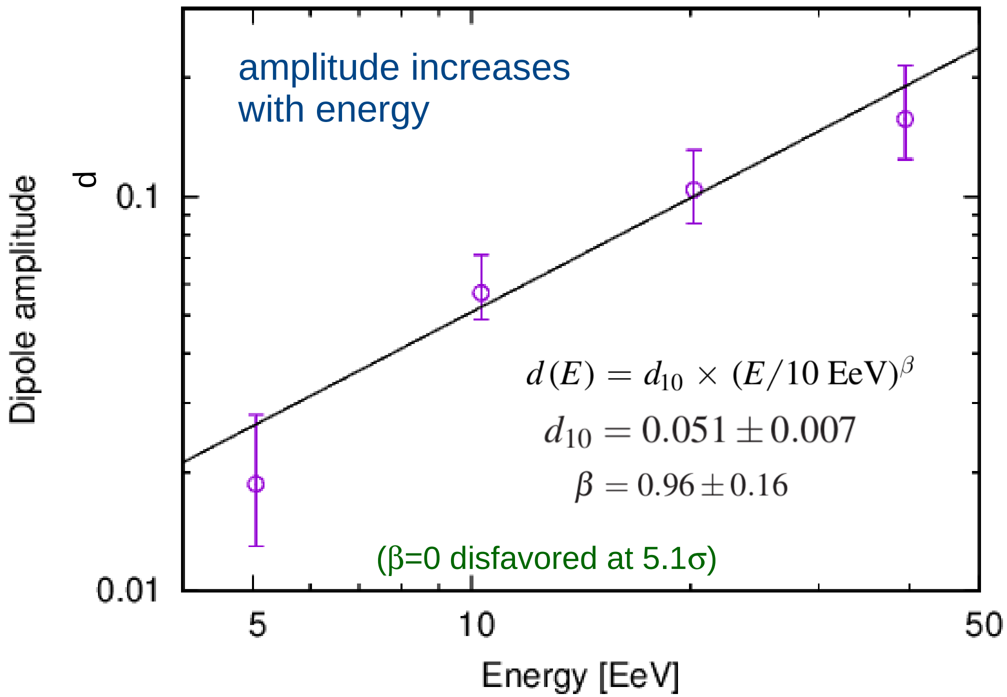

dipole direction away from Galactic Center

close to outer spiral arm in all E bins above 4 EeV

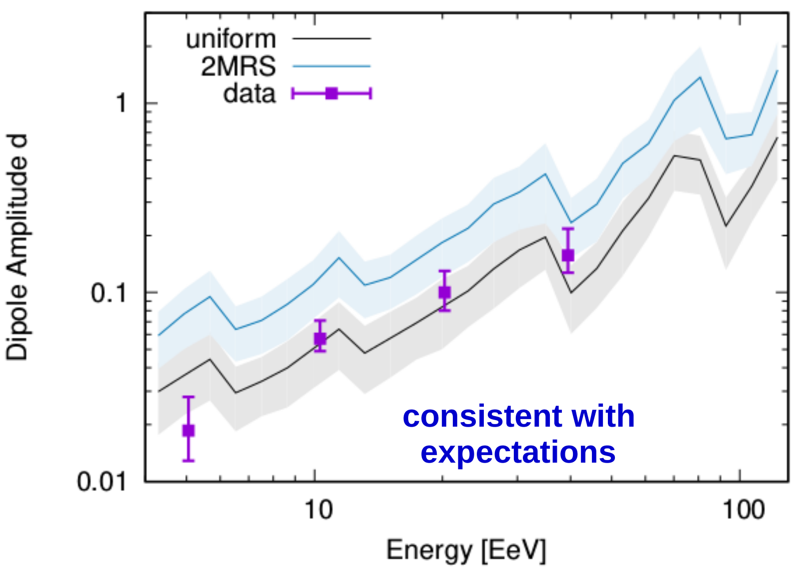

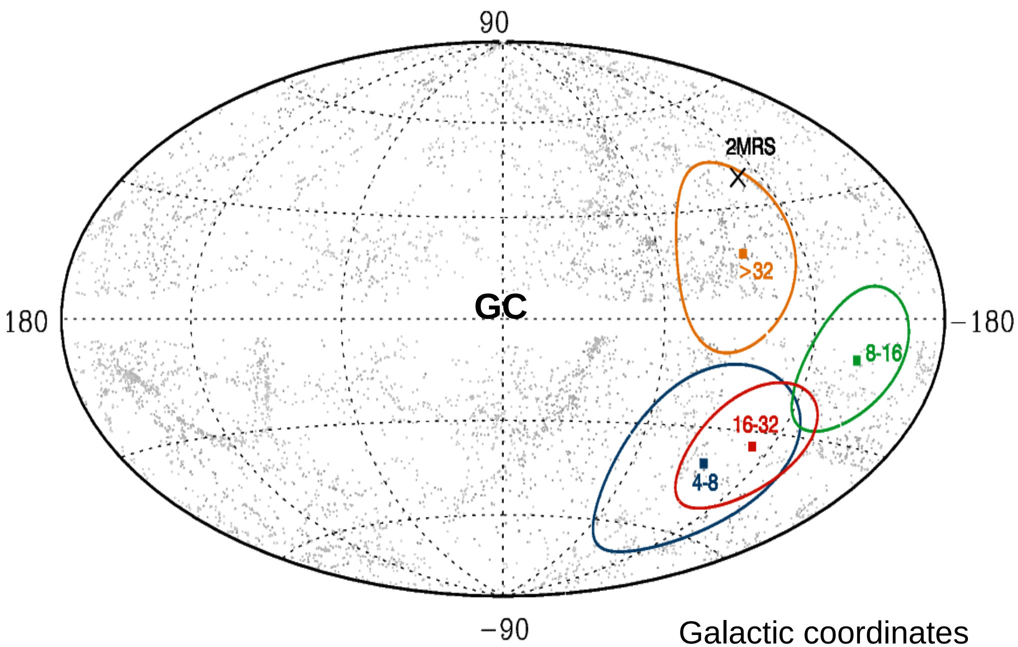

Galactic coordinates

[models with source density 10^{-4} Mpc^{-3} from PRD92 (2015) 063014]

Effect of Galactic B field on extragalactic dipole direction (and amplitude)

ApJ 868 (2018) 4

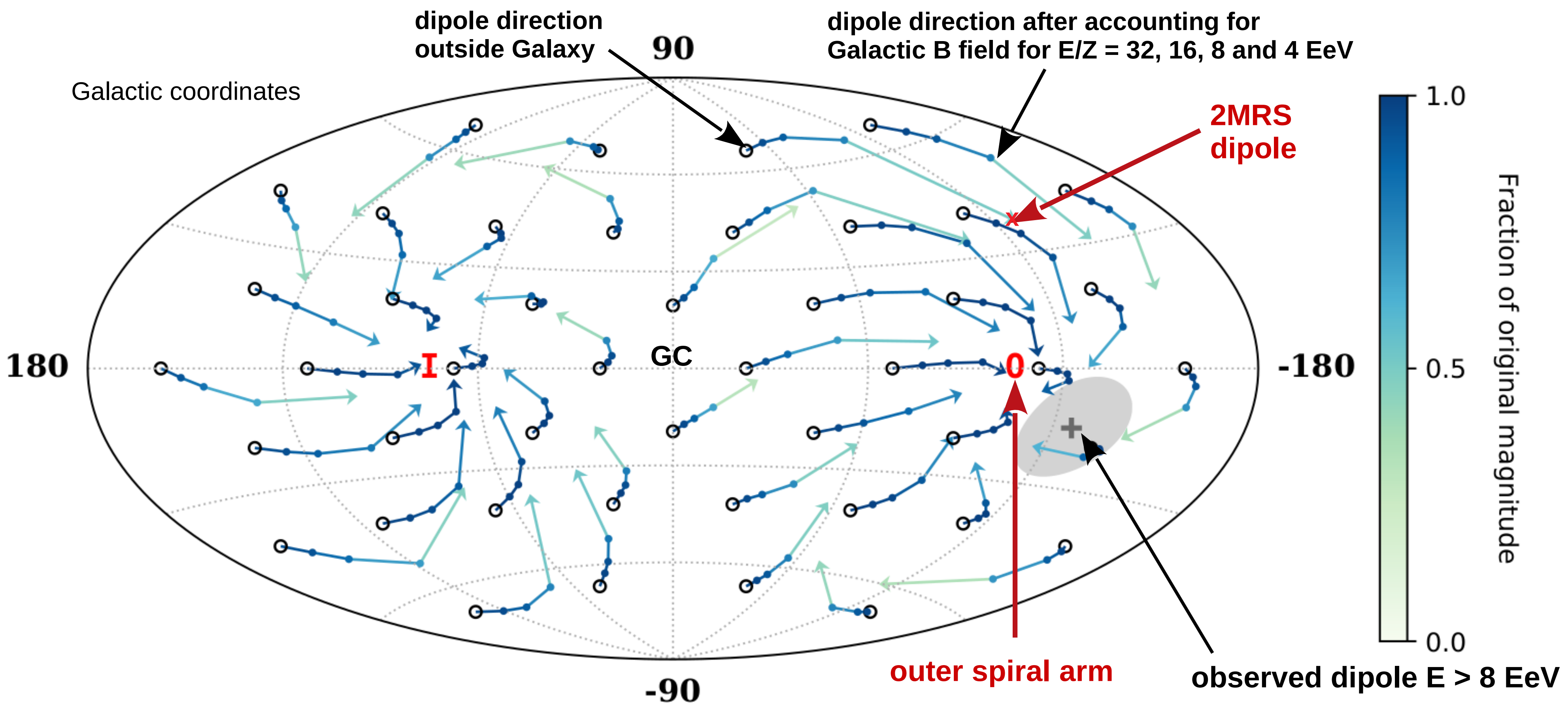

(using Jansson&Farrar 2012 B field model)

extragalactic dipole direction gets shifted towards spiral arms by Galactic B field

LARGE SCALE ANISOTROPY

Auger
E> 8 EeV

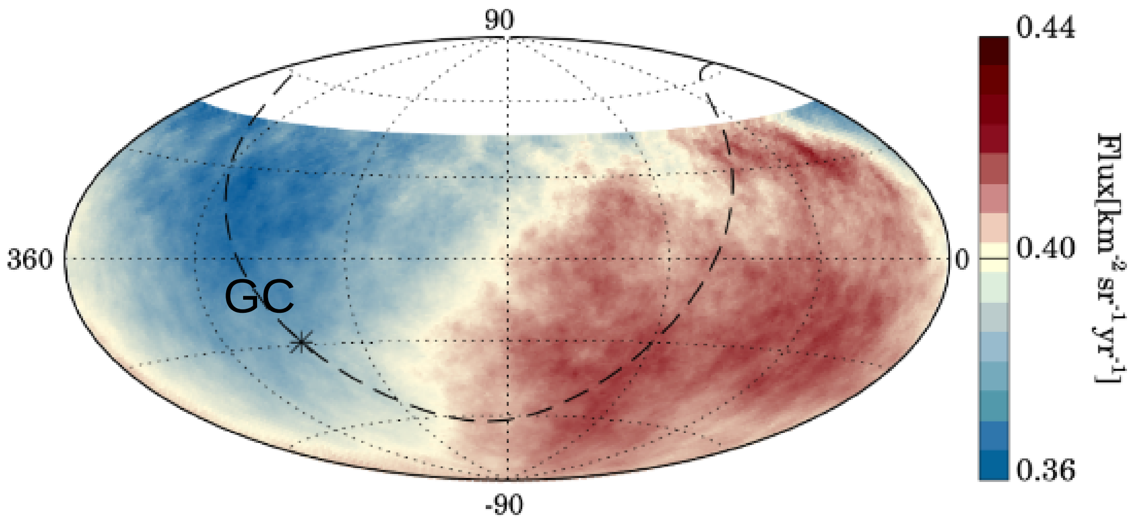

TA
E>10 EeV

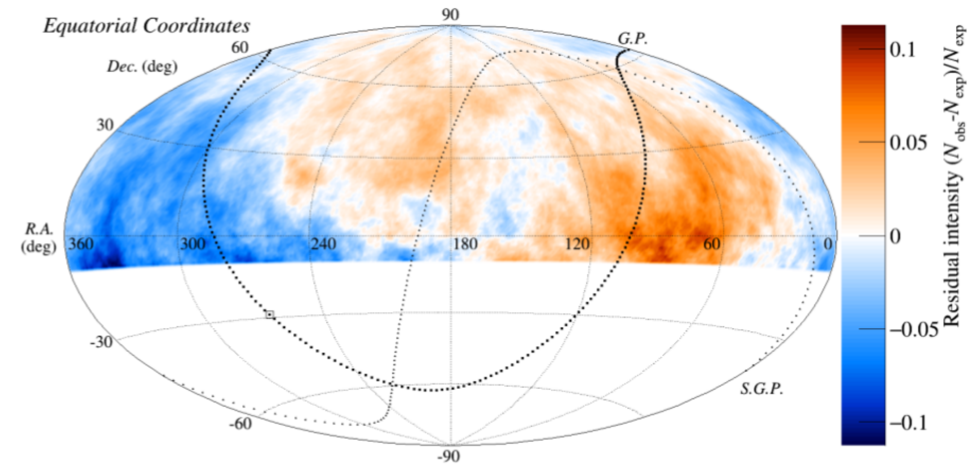

Dipole amplitude $d=0.066^{+0.012}_{-0.009}$ (6σ) pointing to $(\alpha,\delta)=(98^o,-25^o)$ → at 125^o from the GC
→ evidence of extragalactic origin

$d_\perp=0.060\pm0.010$

$r=0.033\pm0.019$ $\phi=131^o\pm33^o$
compatible with Auger dipole
and with isotropy

$d_\perp=r/\langle\cos\delta\rangle \sim 1.3\ r \sim 0.043\pm 0.025$

E Roulet (Auger coll) ICRC 2019

TA coll, arXiv:2007.00023

Modulation in right ascension from 0.03 EeV up to > 32 EeV

Use Fourier analysis in RA for E > 2 EeV

below 2 EeV, non-negligible amplitudes at anti-sidereal frequency suggest possible leftover systematics could be present at sidereal frequency

Use East-West method below 2 EeV (uncertainties larger but always safe)

systematic effects are the same in East & West sectors
→ difference between both rates gives clean measurement of derivative of modulation from which the actual modulation can be recovered
- E-W has smaller sensitivity than usual Fourier analysis

use SD1500 array and E-W for 0.25 EeV < E < 2 EeV ($\theta < 60°$)

For E < 0.25 EeV, smaller SD750 array has actually better sensitivity

use SD750 array and E-W for 0.03 EeV < E < 0.25 EeV ($\theta < 55°$)

$$a_{\rm EW} = \frac{2}{N}\sum_{i=1}^{N}\cos(\alpha^0(t_i) - \xi_i)$$

$$b_{\rm EW} = \frac{2}{N}\sum_{i=1}^{N}\sin(\alpha^0(t_i) - \xi_i)$$

$$r_{\rm EW} = \sqrt{a_{\rm EW}^2 + b_{\rm EW}^2}$$

$$\varphi_{\rm EW} = \arctan(b_{\rm EW}/a_{\rm EW})$$

$$\xi_i = \begin{cases} 0 & east \\ \pi & west \end{cases}$$

$$r = \frac{\pi\langle\cos\delta\rangle}{2\langle\sin\theta\rangle} r_{\rm EW}$$

$$\varphi = \varphi_{\rm EW} + \pi/2$$

Fourier analysis

EQUATORIAL DIPOLE FROM 1 PeV TO 100 EeV

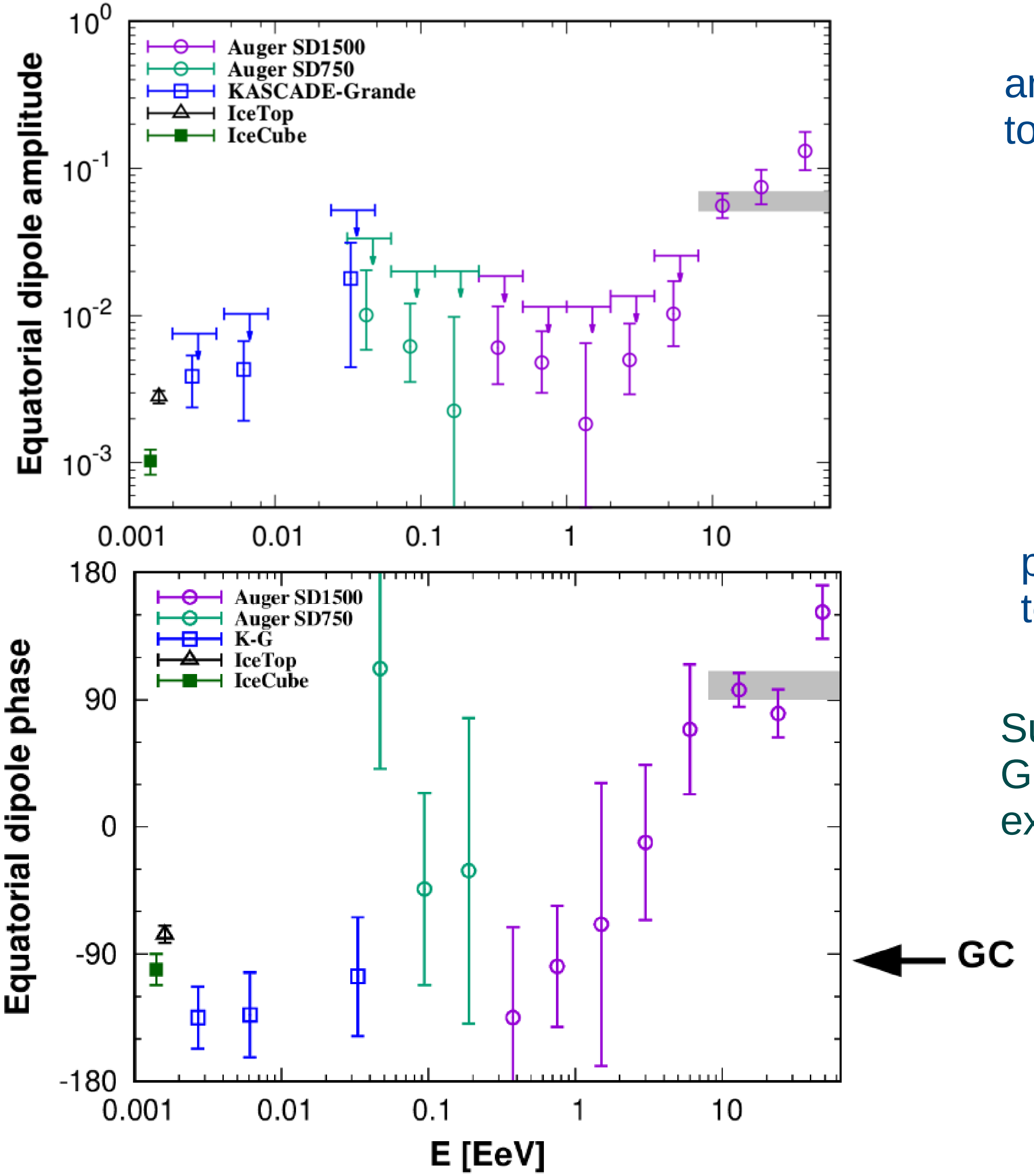

amplitudes grow, from below 1% to above 10%

phases shift, from ~ GC to ~ opposite direction

Suggests transition from anisotropies of Galactic origin below ~1 EeV to extragalactic origin above few EeV

Auger coll, ApJ 891(2020)

EQUATORIAL DIPOLE RESULTS

	E [EeV]	N	$d_\perp$	$\alpha_d [^\circ]$	$P(\geq d_\perp)$	$d_\perp^{99}$	$d_\perp^{\rm UL}$
East-West (SD750)	0.03125 - 0.0625	432,155	$0.010^{+0.010}_{-0.004}$	112 ± 71	0.54	0.028	0.033
	0.0625 - 0.125	924,856	$0.006^{+0.006}_{-0.003}$	-44 ± 68	0.50	0.016	0.020
	0.125 - 0.25	488,752	$0.002^{+0.008}_{-0.002}$	-31 ± 108	0.94	0.019	0.020
East-West (SD1500)	0.25 - 0.5	770,316	$0.006^{+0.005}_{-0.003}$	-135 ± 64	0.45	0.015	0.018
	0.5 - 1.0	2,388,467	$0.005^{+0.003}_{-0.002}$	-99 ± 43	0.20	0.008	0.011
	1 - 2	1,243,103	$0.0018^{+0.0047}_{-0.0002}$	-69 ± 100	0.87	0.011	0.011
Fourier (SD1500)	2 - 4	283,074	$0.005^{+0.004}_{-0.002}$	-11 ± 55	0.34	0.010	0.014
	4 - 8	88,325	$0.010^{+0.007}_{-0.004}$	69 ± 46	0.23	0.018	0.026
	8 - 16	27,271	$0.056^{+0.012}_{-0.010}$	97 ± 12	2.3×10^{-6}	0.033	–
	16 - 32	7,664	$0.075^{+0.023}_{-0.018}$	80 ± 17	1.5×10^{-3}	0.063	–
	≥ 32	1,993	$0.13^{+0.05}_{-0.03}$	152 ± 19	5.3×10^{-3}	0.12	–
	≥ 8	36,928	$0.060^{+0.010}_{-0.009}$	98 ± 9	1.4×10^{-9}	0.028	–

99 %CL upper-bounds

SEARCH FOR OVERDENSITIES AT THE HIGHEST ENERGIES (E > 32 EeV)

Blind search - whole sky 1°x 1°grid
Scan:
$1° \leq \psi \leq 30°$
$32\ \text{EeV} \leq E_{th} \leq 80\ \text{EeV}$
2157 events

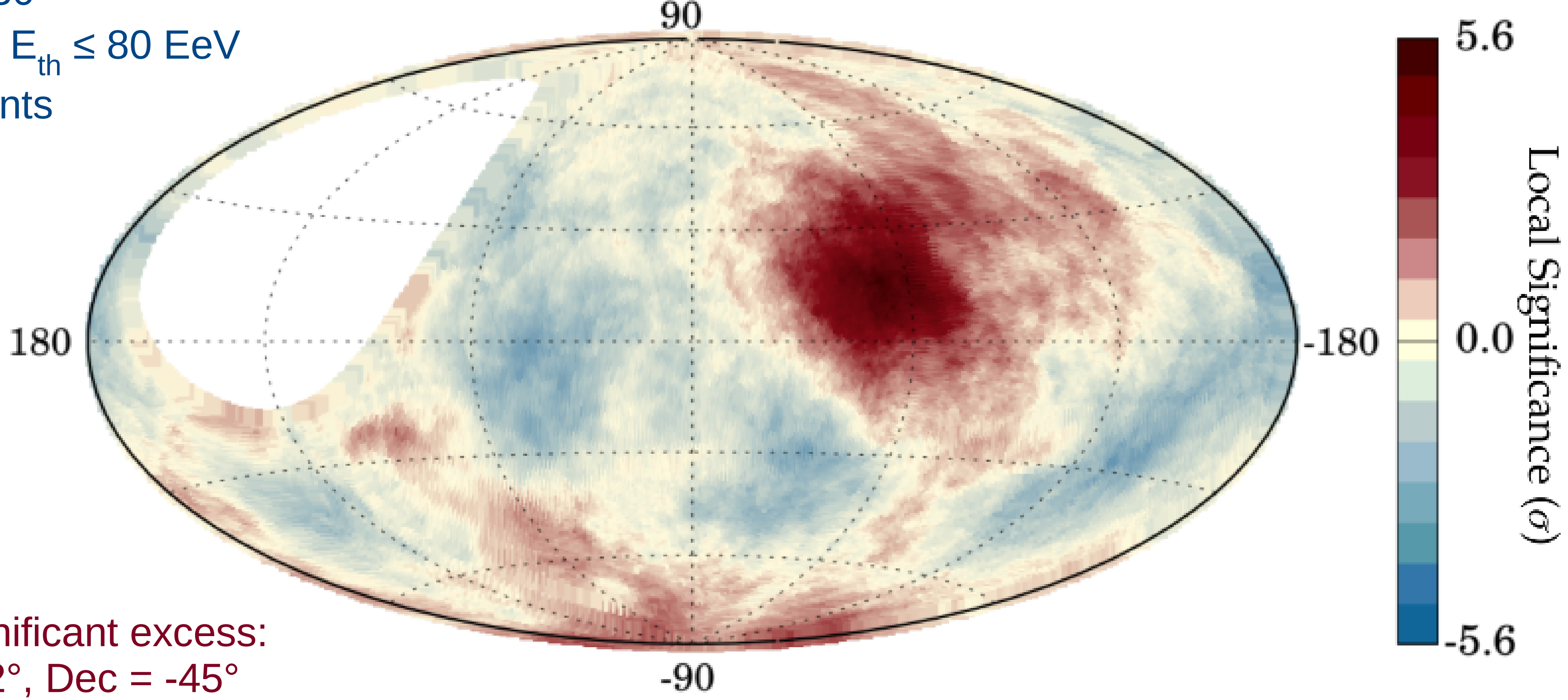

Most significant excess:
RA = 202°, Dec = -45°
(l,b) = (310°,17°)
E_{th} = 38 EeV
ψ = 27°
N_{obs} = 188, n_{exp} = 125
local Li-Ma significance=5.6σ
post-trial p-value=2.5%

The Centaurus A region

ICRC 2019

Cen A is the closest radiogalaxy
D ~ 3.6 Mpc

Scan:
1° ≤ ψ ≤ 30°
32 EeV ≤ E_{th} ≤ 80 EeV

Most significant excess:
E_{th} = 37 EeV
ψ = 28°
N_{obs} = 203, n_{exp} = 141
local p-value=1.5x10^{-7}
post-trial: 3.9 σ

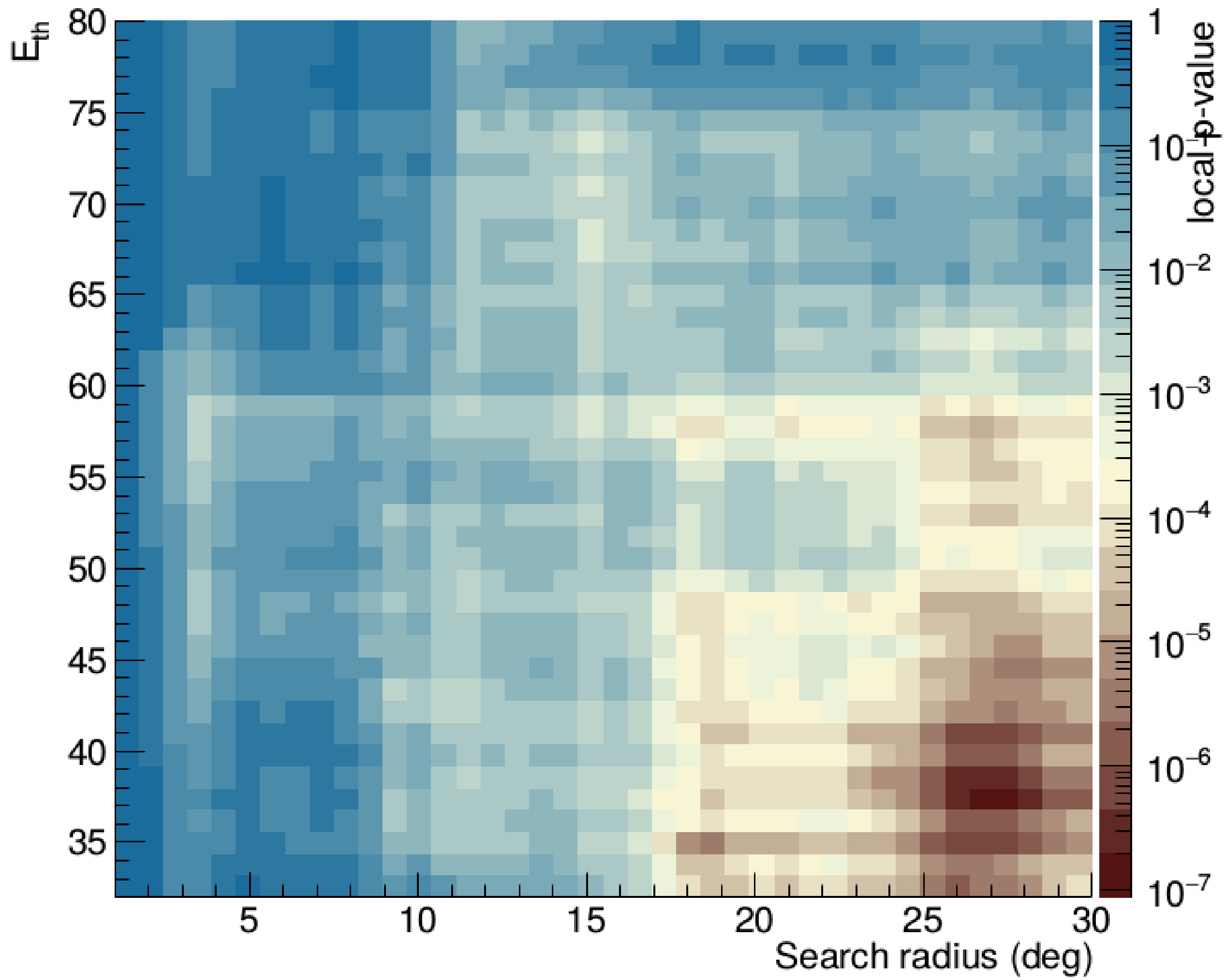

MEDIUM-SCALE ANISOTROPIES AT THE HIGHEST ENERGIES

- full sky analysis combining Auger & TA data (E_{Auger} ≥ 40 EeV, E_{TA} ≥ 53.2 EeV)

- Scan over circular windows with 7 radii (5° , 10° , . . . , 35°), 49 152 centers (≈ 0.9° HEALPix grid)

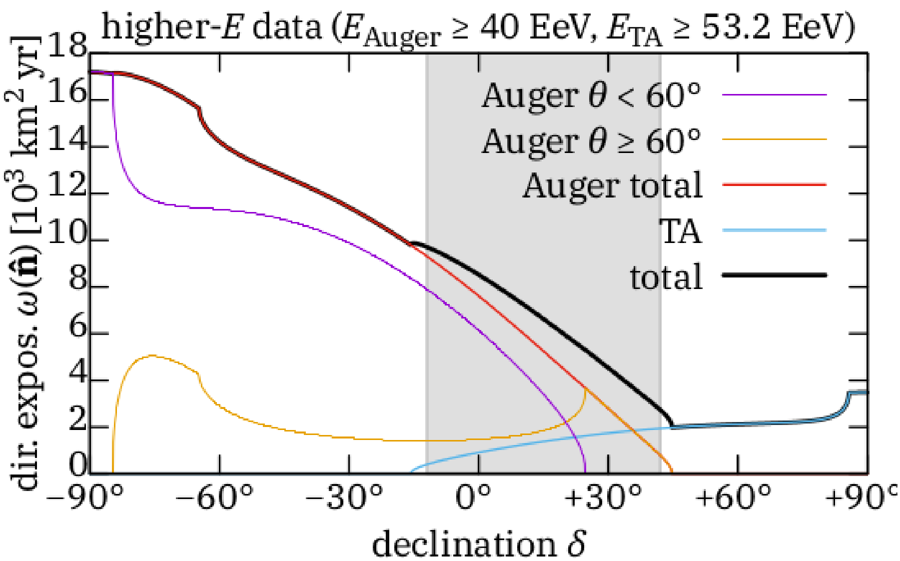

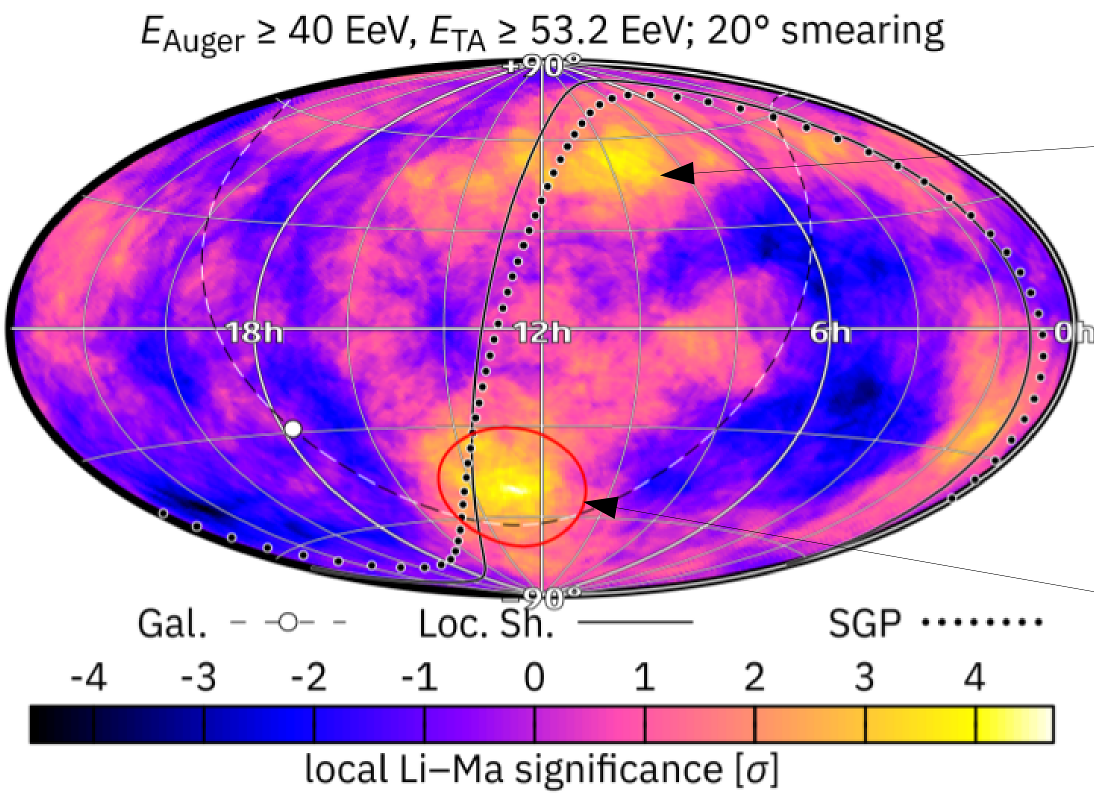

15° radius around (α,δ)=(142°, +54°)
4.2σ pre-trial (1.5σ post-trial)

20° radius around (α,δ)=(192°, −50°)
4.7σ pre-trial (2.2σ post-trial)

A. di Matteo et al. (Auger and TA colls.), ICRC 2019

Likelihood test for anisotropy with astrophysical catalogs

- Take into account that brighter objects are expected to contribute more to the flux
- account for attenuation due to CR interactions

Likelihood Method

Probability maps:
- Weight objects by their relative flux in the corresponding electromagnetic wavelength
- Different attenuation due to different distances to sources taken into account
- A smearing angle θ around each object to take into account magnetic deflections ➤ First free parameter
- Source fraction (rest isotropic) ➤ Second free parameter (f_{aniso})
- Directional exposure normalized to the total number of events

Test statistic defined as the ratio of likelihoods: $TS = 2 \log [L(\psi, f_{aniso}) / L(f_{aniso} = 0)]$

Scan in energy thresholds 32 EeV ≤ Eth ≤ 80 EeV [1 EeV steps]

Test 4 different catalogs:
- **γ-emitting AGNs:** selected using Fermi 3FHL weighted by Φ(E>10 GeV) → 33 sources (including Cen A, Fornax A, M87, Mkn421): mostly blazars and FR-I radio-galaxies

- **Starburst Galaxies:** weighted by Φ(1.4 Ghz), selected from Ackermann+ 12 and Becker+ 09 , with data from HEASARC Radio Master Catalog, 32 sources (including NGC4945, NGC253, Circinus, M82 M83…)

- **Swift-BAT:** weighted by Φ(14−195 keV), both radio loud and quiet AGNs , >300 sources

- **2MRS:** weighted by Φ(k-band), traces local matter (some 10^4 sources), Local group excluded (D>1Mpc)

Likelihood test for anisotropy with astrophysical catalogs

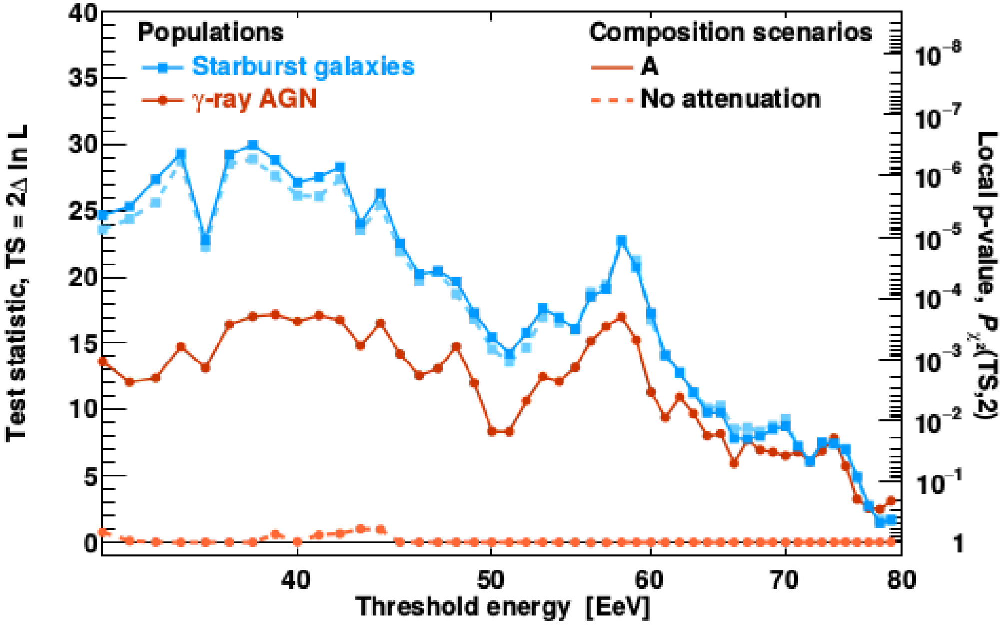

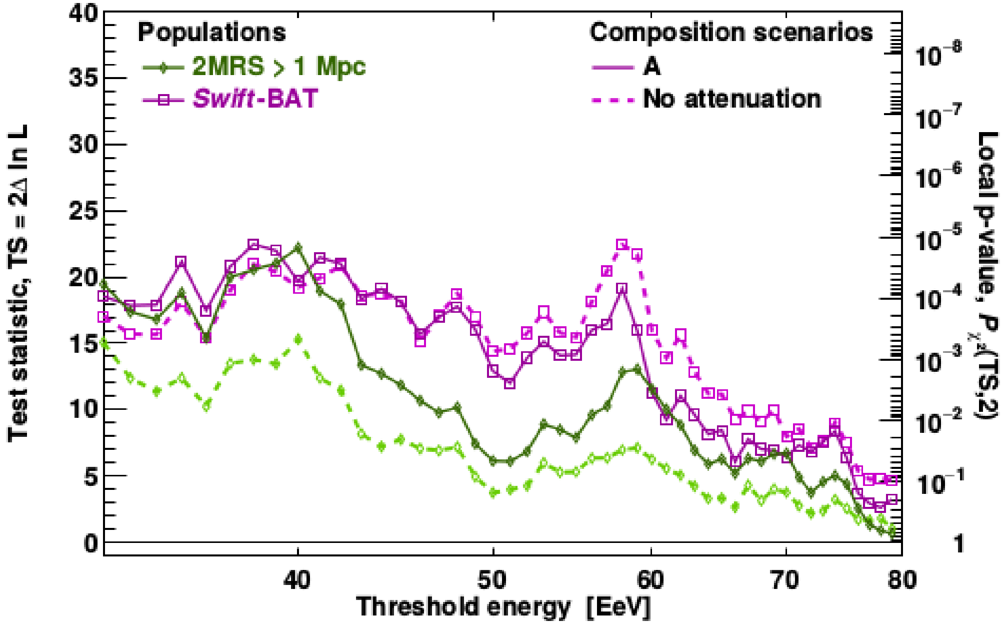

Catalog	$E_{\rm th}$	TS	Local p-value	post-trial	$f_{\rm aniso}$	θ
Starburst	38 EeV	29.5	4×10^{-7}	4.5 σ	$11^{+5}_{-4}\%$	$15^{+5}_{-4}{}^\circ$
γ–AGN	39 EeV	17.8	1×10^{-4}	3.1 σ	$6^{+4}_{-3}\%$	$14^{+6}_{-4}{}^\circ$
Swift-BAT	38 EeV	22.2	2×10^{-5}	3.7 σ	$8^{+4}_{-3}\%$	$15^{+6}_{-4}{}^\circ$
2MRS	40 EeV	22.0	2×10^{-5}	3.7 σ	$19^{+10}_{-7}\%$	$15^{+7}_{-4}{}^\circ$

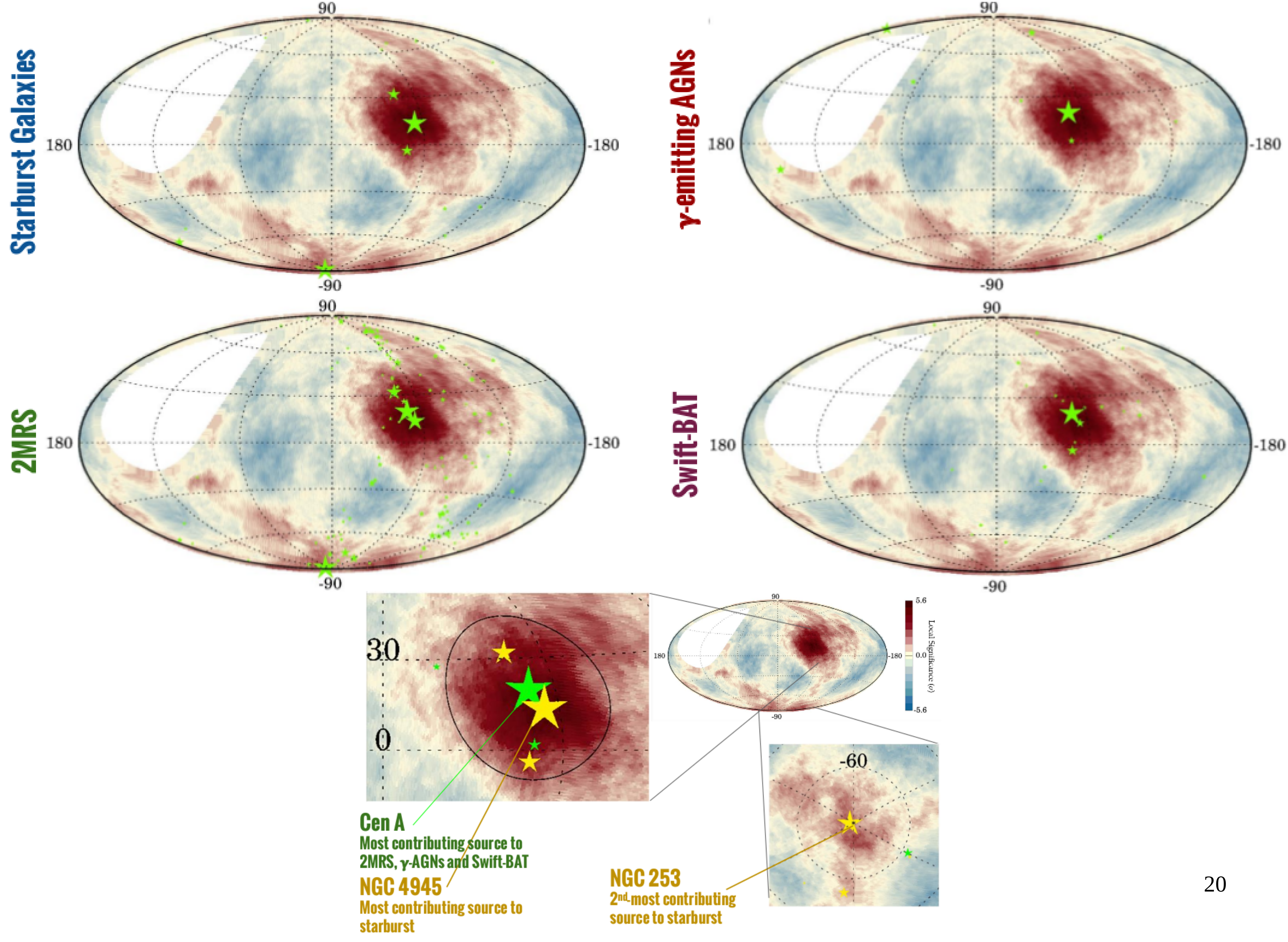

Starburst Galaxies
γ-emitting AGNs
2MRS
Swift-BAT
90
180
-180
-90
30
0
-60
5.6
0.0
-5.6
Local Significance (σ)
Cen A
Most contributing source to 2MRS, γ-AGNs and Swift-BAT
NGC 4945
Most contributing source to starburst
NGC 253
2nd most contributing source to starburst

ANISOTROPIES SEARCH SUMMARY:

- dipolar modulation of 6.6 % amplitude for E > 8 EeV
- Hints of Intermediate angular scale anisotropy at ~40 EeV
- No evidence of small scale anisotropies

→ PROBABLY INDICATING LARGE DEFLECTIONS IN INTERGALACTIC B FIELD (consistent with heavy composition at highest energies)

ORIGIN OF THE DIPOLE

- Too large amplitude to be Compton-Getting

- Local matter inhomogeneously distributed:
if CR sources save a similar distribution → dipole of CR expected

- If intergalactic MF large and/or Z sufficiently large, CR can propagate diffusively in XGMF → dipolar anisotropy in direction of the closest source(s)

Propagation in turbulent XGMF: spectrum and arrival direction significantly affected

B: rms amplitude, l_c: coherence length

Critical energy $r_L(E_c) = l_c$ → for $E < E_c$ large deflections for distances $< l_c$

$$r_{\rm L} = \frac{E}{ZeB}$$

Larmor radius

$$E_{\rm c} = ZeBl_{\rm c} \simeq 0.9Z \frac{B}{\rm nG} \frac{l_{\rm c}}{\rm Mpc}\,{\rm EeV}$$

Kolmogorov
m=5/3

Diffusion length: deflection ~1 rad

$$l_D(E) \simeq l_c \left[4\left(\frac{E}{E_c}\right)^2 + a_I\left(\frac{E}{E_c}\right) + a_L\left(\frac{E}{E_c}\right)^{2-m}\right]$$

For a source at distance r_s

$l_D(E) \simeq r_s$

E

Diffusion — Quasi rectilinear

Angular distribution wrt the source direction

$$\langle\cos\theta\rangle = \frac{1}{3R}\left[1 - \exp\left(-3R - \frac{7}{2}R^2\right)\right] \equiv C(R) \rightarrow \begin{cases} 1 - r_s/3\,l_D & r_s \ll l_D \\ l_D/3r_s & r_s \gg l_D \end{cases}$$

$$R \equiv r_s/l_D$$

Harari MR 2014

Flux from one source: diffusion leads to enhancement of the density around it

Steady source

$$n(E, r_s) 4\pi r_s^2 c \langle \cos\theta(E, r_s) \rangle = Q(E)$$

density enhanced wrt rectilinear propagation by

$$\xi \equiv \frac{n(E, r_s)}{Q(E)/(4\pi r_s^2 c)} = \frac{1}{\langle \cos\theta \rangle}$$

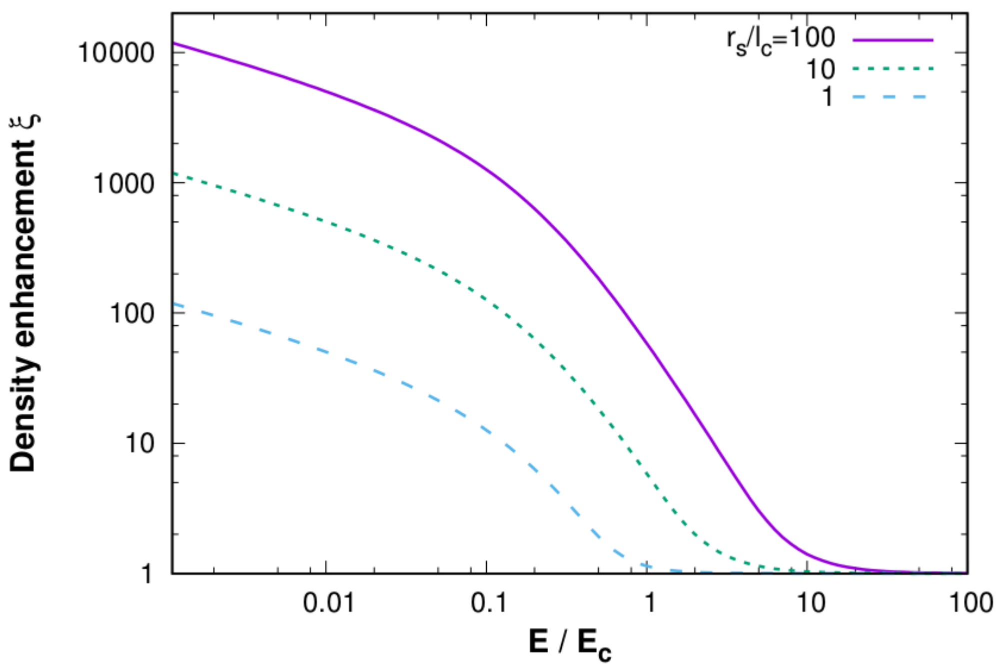

related to dipolar amplitude by

$\Delta = 3 \langle \cos\theta \rangle = 3/\xi$

Finite emission time

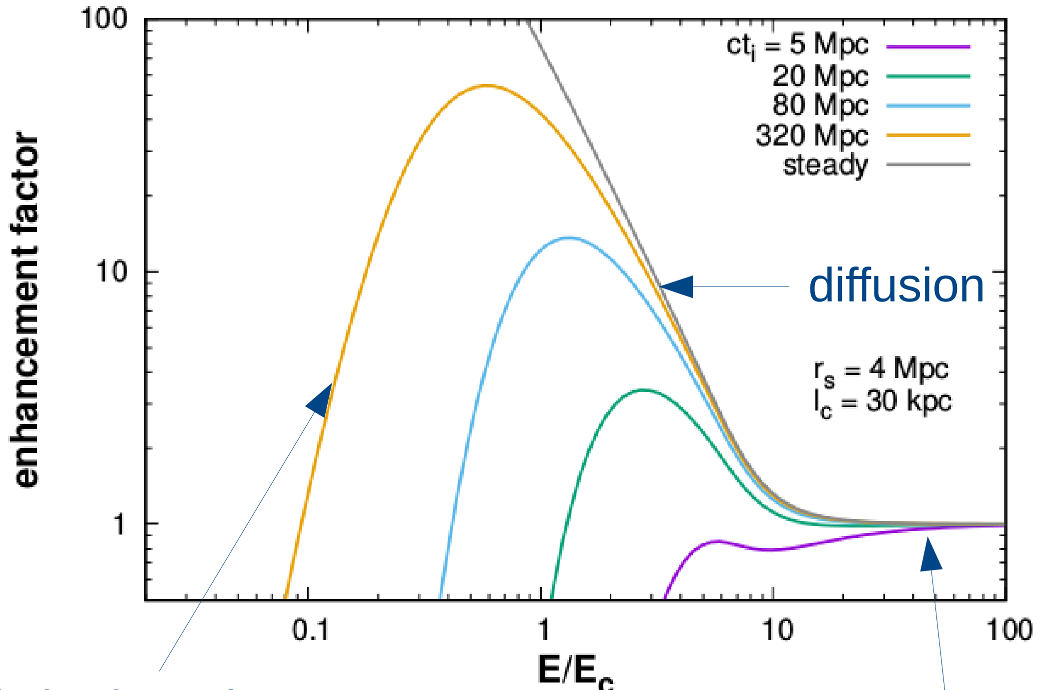

magnetic horizon: low energy particles need longer than the source emitting time to reach r_s

rectilinear propagation

Angular distribution from one source:

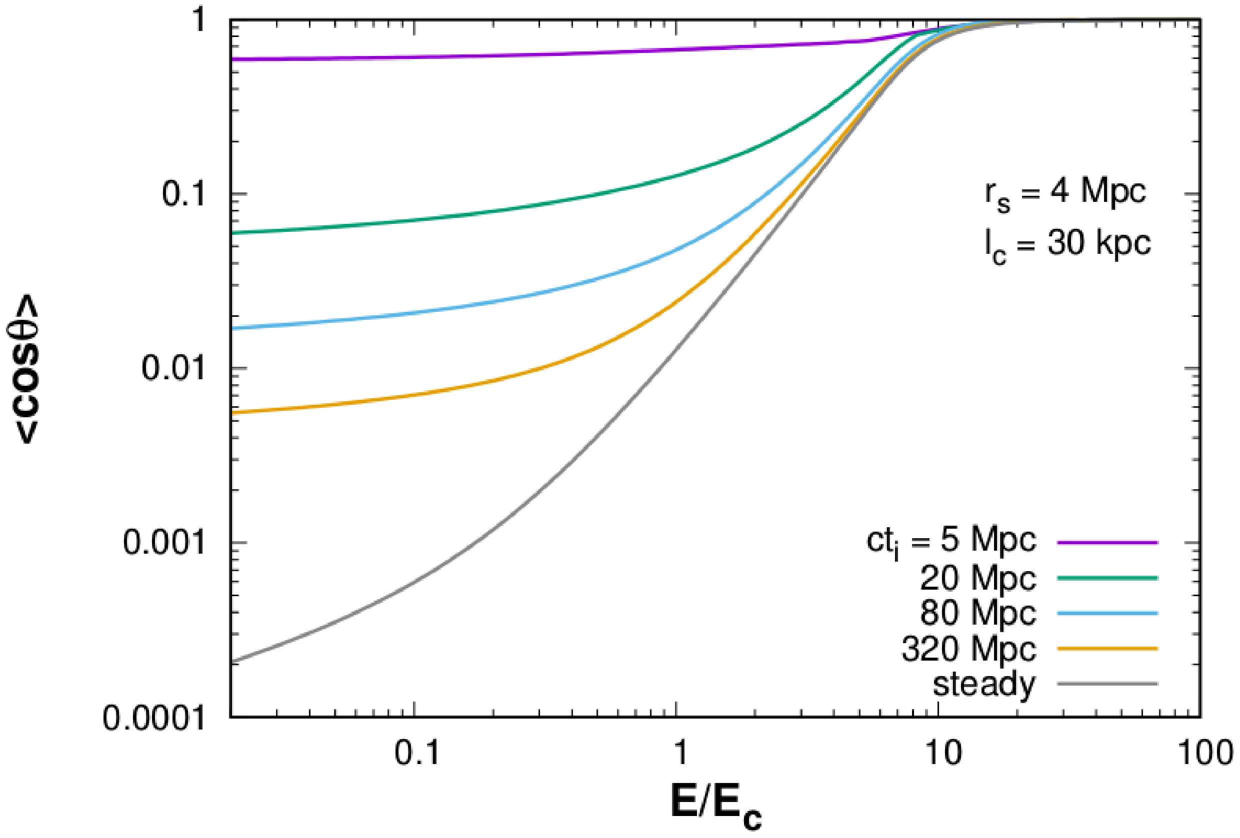

$$E_c = ZeBl_c \simeq 0.9Z \frac{B}{\mathrm{nG}} \frac{l_c}{\mathrm{Mpc}} \,\mathrm{EeV}$$

Dipolar amplitude: $\Delta = 3 \langle \cos\theta \rangle$

Dipole amplitude from a distribution of sources

$$\vec{\Delta}(E) = \sum_{i,j} \frac{f_j n_i^{(j)}}{n_t} \vec{\Delta}_i^{(j)}(E) \qquad n_t(E) = \sum_{i,j} f_j n_i^{(j)}(E)$$

mixed composition scenario

E_{max} = Z 6 EeV, γ= 2

$(f_p,f_{He},f_C,f_{Si},f_{Fe})=(0.19,0.19,0.4,.19,0.03)$

homogeneous distribution of sources

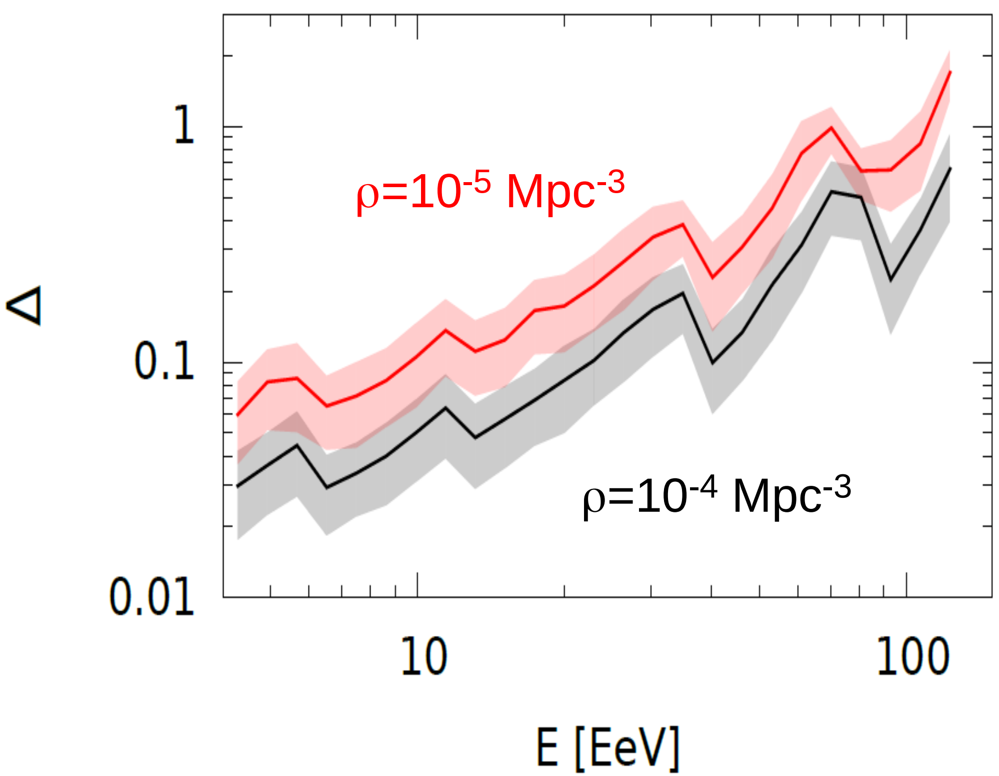

ρ=10-4 Mpc-3

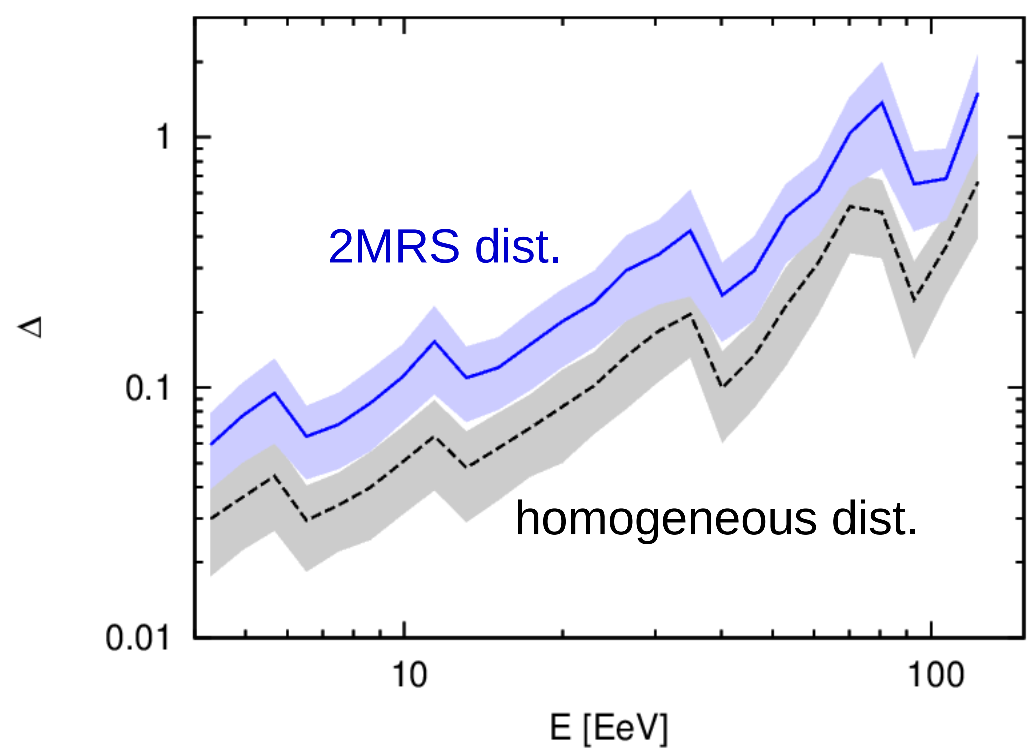

- Dipole amplitude expected to increase with energy
- few % dipole amplitude at 10 EeV can easily arise

Harari, SM, Roulet, PRD 2015

SUMMARY

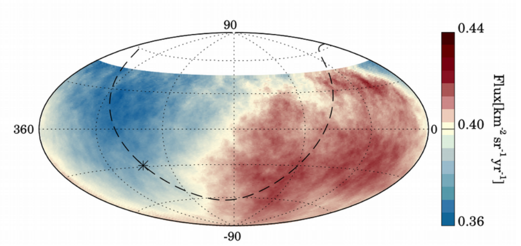

- LSA in the bin above 8 EeV has the most significant departure from isotropy, with $d = 0.066^{+0.012}_{-0.008}$ and 125^o away from GC, indicative of an extragalactic origin

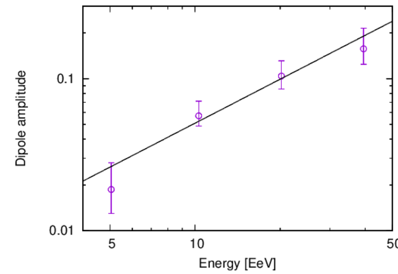

- dipole amplitude above 4 EeV grows with energy

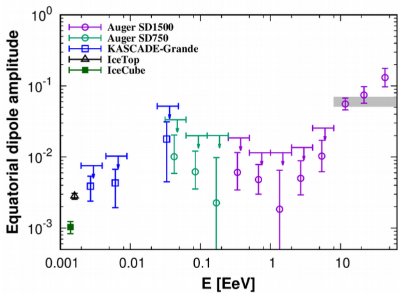

- dipole amplitudes below 8 EeV are not significant
  99% CL upper bounds on $d_\perp$ are at the level of 1 to 3%

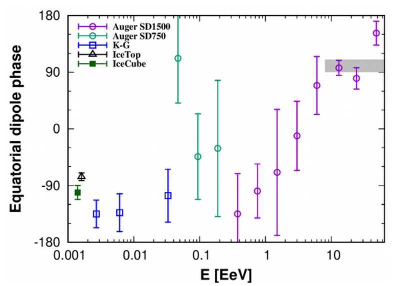

- RA phases suggest that anisotropy has a predominantly Galactic origin below 1 EeV and a predominantly extragalactic origin above few EeV

- Most significant overdensity: (l,b) = (310°,17°)
  E_{th} = 38 EeV, ψ = 27°, local Li-Ma: 5.6σ (post-trial p-value=2.5%)

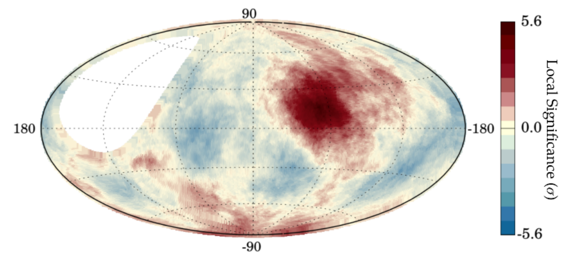

- Centaurus A: most significant excess at E_{th} =37 EeV ψ= 28°
  (3.9 σ post-trial significance)

- Starburst Galaxies: best rejection of pure isotropic hypothesis at
  E_{th} = 38 EeV, f_{aniso} = 11%, θ= 15° (4.5 σ post-trial significance)
  The region around the most significant excess is populated by a number of highly contributing candidate sources in the considered catalogs

BACKUP

Model Excess Map

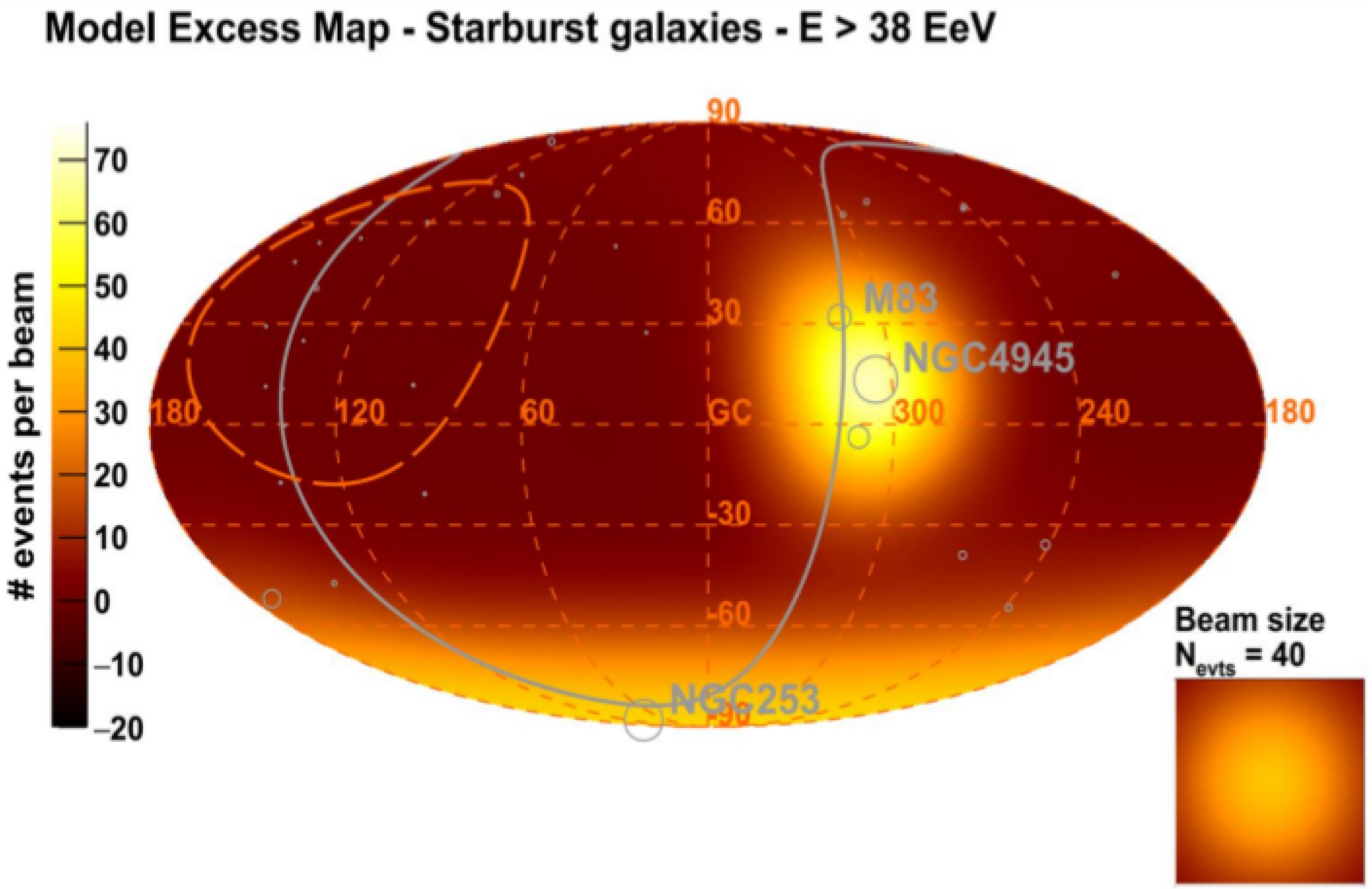

Sources most contributing to the likelihood analysis

Starburst Galaxies

Src	l	b	excess-weight
NGC4945	305.27	13.34	100.0%
NGC253	97.36	-87.97	77.7%
M83	314.58	31.97	27.7%
Circinus	311.33	-3.81	22.4%
NGC1068	172.10	-51.93	14.8%
NGC1808	241.21	-35.90	3.8%
NGC1672	268.78	-38.99	2.8%
NGC4631	142.81	84.22	2.2%
NGC1365	237.96	-54.60	2.1%
NGC4666	299.54	62.37	1.3%
M61	284.37	66.28	1.3%
NGC3627	241.96	64.42	1.3%
NGC2903	208.71	44.54	1.2%
M51	104.85	68.56	1.1%
NGC660	141.61	-47.35	1.1%
NGC3628	240.85	64.78	1.1%

γ-emitting AGNs

Src	l	b	excess-weight
CenA	309.52	19.42	100.0%
Mkn421	179.83	65.03	22.6%
NGC1275	150.58	-13.26	14.2%
FornaxA	240.16	-56.69	11.0%
M87	283.78	74.49	11.0%
CenB	309.72	1.73	7.3%
Mkn501	63.60	38.86	5.7%
APLibrae	340.68	27.58	2.3%
PMNJ0816-1311	234.80	12.12	1.6%

Swift-BAT

Src	l	b	excess-weight
CenA	309.52	19.42	100.0%
Circinus	311.33	-3.81	18.0%
NGC4945	305.27	13.34	12.9%
NGC2110	212.93	-16.55	3.8%
NGC6300	328.49	-14.05	3.3%
NGC5506	339.15	53.81	3.2%
MCG-05-23-016	262.74	17.23	3.0%
NGC7172	15.13	-53.07	2.5%
NGC3783	287.46	22.95	2.5%
NGC4507	299.64	22.86	2.1%
IC4329A	317.50	30.92	2.1%
NGC4388	279.12	74.34	2.1%
NGC7582	348.08	-65.70	1.9%
NGC4151	155.08	75.06	1.8%
ESO103-035	329.78	-23.18	1.4%
NGC1365	237.96	-54.60	1.4%
NGC6814	29.35	-16.01	1.3%
4U1344-60	309.77	1.51	1.3%
NGC3081	259.02	25.03	1.2%
NGC7314	27.14	-59.74	1.1%
NGC3227	216.99	55.45	1.1%
NGC3281	273.01	19.78	1.1%
NGC5728	337.32	38.10	1.1%
MCG-06-30-015	313.29	27.68	1.0%

Allowing also for the presence of quadrupolar components

Dipole and quadrupole components in the two energy bins. The x axis is in the direction $\alpha = 0°$

Energy [EeV]	d_i	Q_{ij}
4 - 8	$d_x = -0.001 \pm 0.008$	$Q_{zz} = -0.003 \pm 0.039$
	$d_y = 0.008 \pm 0.008$	$Q_{xx} - Q_{yy} = -0.004 \pm 0.028$
	$d_z = -0.014 \pm 0.022$	$Q_{xy} = 0.006 \pm 0.014$
		$Q_{xz} = -0.008 \pm 0.018$
		$Q_{yz} = -0.005 \pm 0.018$
≥ 8	$d_x = -0.004 \pm 0.012$	$Q_{zz} = 0.032 \pm 0.061$
	$d_y = 0.054 \pm 0.012$	$Q_{xx} - Q_{yy} = 0.077 \pm 0.048$
	$d_z = -0.011 \pm 0.035$	$Q_{xy} = 0.038 \pm 0.024$
		$Q_{xz} = 0.015 \pm 0.029$
		$Q_{yz} = -0.016 \pm 0.029$

no significant quadrupolar components
→ dipolar amplitudes consistent with dipole only results

Expected “hot spot” from the closest source: nuclei

B_{rms} = 1 nG
L_c = 1 Mpc
spectrum E^{-2}

E_{max} = Z 6 EeV, γ= 2, $(f_p,f_{He},f_C,f_{Si},f_{Fe})$=(0.19,0.19,0.4,.19,0.03)

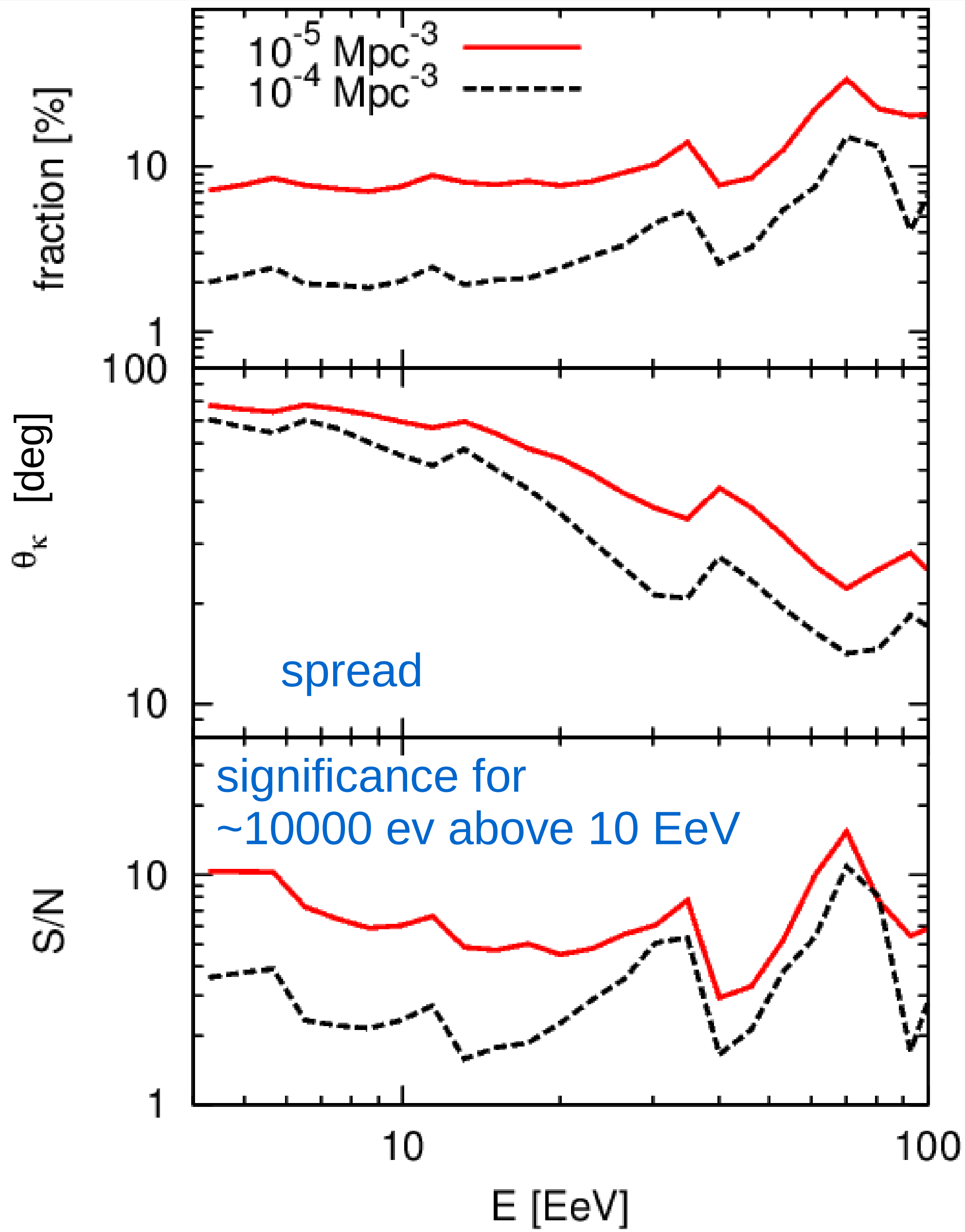

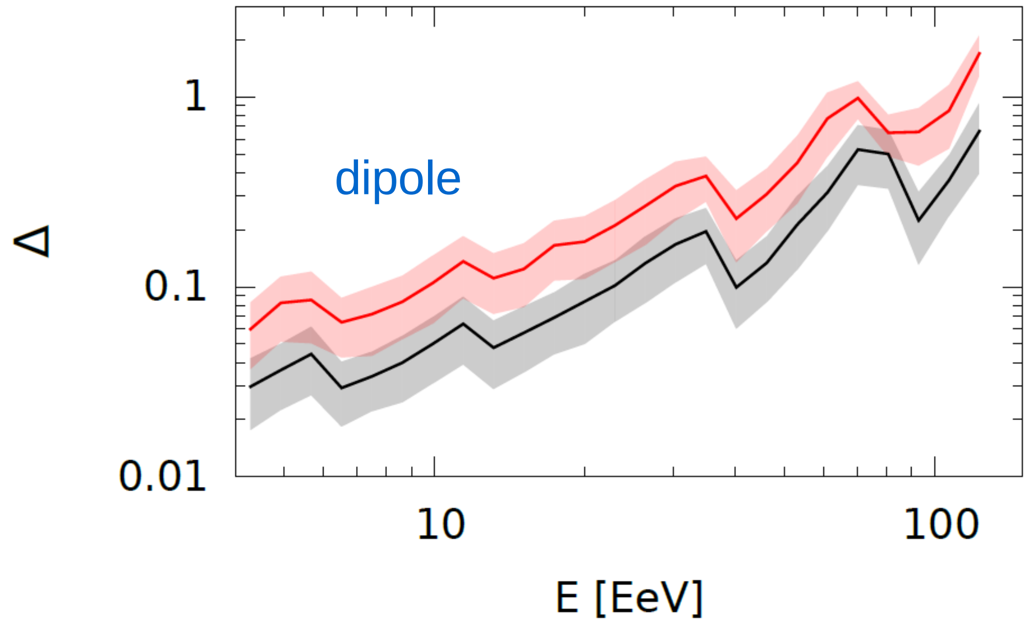

angle between hot spot and dipole

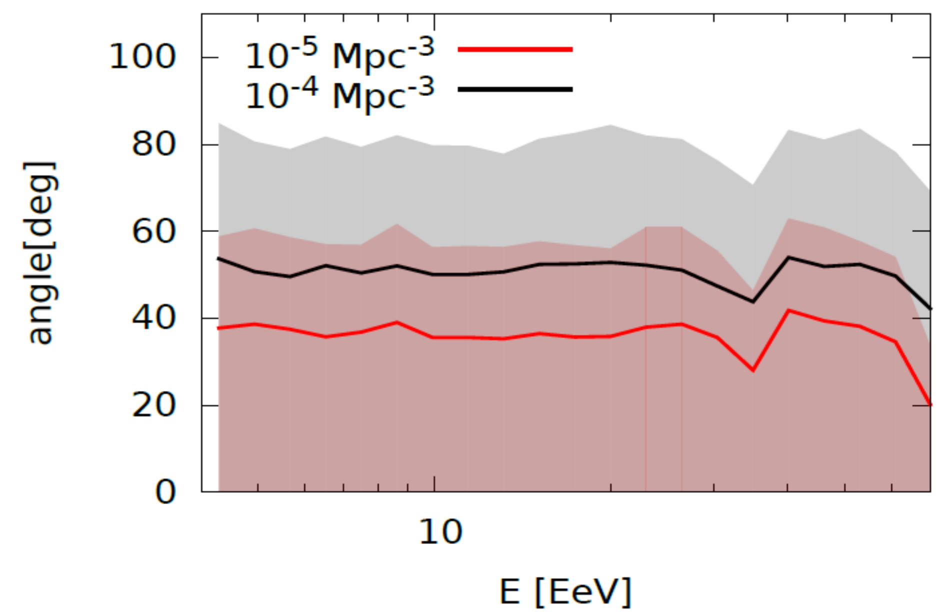

For $\rho=10^{-4}$ Mpc^{-3} hot spot at 15-20 deg and 3-5 sigma significance